Title

Continuous Effector CD8+ T Cell Production in a Controlled Persistent Infection Is Sustained by a Proliferative Intermediate Population

Journal

Immunity, 45(1)

ISSN

1074-7613

Authors

Chu, H Hamlet
Chan, Shiao-Wei
Gosling, John Paul
et al.

Publication Date

2016-07-01

DOI

10.1016/j.immuni.2016.06.013

Peer reviewed

HHS Public Access

Author manuscript

Immunity. Author manuscript; available in PMC 2017 July 19.

Published in final edited form as:

Immunity. 2016 July 19; 45(1): 159–171. doi:10.1016/j.immuni.2016.06.013.

Continuous effector T cell production in a controlled persistent infection is sustained by a proliferative subset of memory-effector hybrid phenotype

H. Hamlet Chu[1,5], **Shiao-Wei Chan**[1], **John Paul Gosling**[2], **Nicolas Blanchard**[3], **Alexandra Tsitsiklis**[1], **Grant Lythe**[4], **Nilabh Shastri**[1], **Carmen Molina-París**[4], and **Ellen A. Robey**[1,5]

[1]Division of Immunology and Pathogenesis, Department of Molecular and Cell Biology, University of California Berkeley, Berkeley, CA 94720, USA

[2]Departments of Statistics, School of Mathematics, University of Leeds, Leeds, UK

[3]Center of Pathophysiology of Toulouse-Purpan, INSERM UMR1043-CNRS UMR5282, University of Toulouse, 31024 Toulouse Cedex 3, France

[4]Departments of Applied Mathematics, School of Mathematics, University of Leeds, Leeds, UK

Summary

Highly functional $CD8^+$ effector T (Teff) cells can persist in large numbers during controlled persistent infections, as exemplified by rare HIV-infected individuals who control the virus. Here we examined the cellular mechanisms that maintain ongoing T effector responses using a mouse model for persistent *Toxoplasma gondii* infection. In mice expressing the protective MHC-I molecule, L^d, a dominant T effector response against a single parasite antigen was maintained without a contraction phase, correlating with ongoing presentation of the dominant antigen. Large numbers of short-lived Teff cells were continuously produced via a proliferative, antigen-dependent intermediate (Tint) population with a memory-effector hybrid phenotype. During an acute, resolved infection, decreasing antigen load correlated with a sharp drop in the Tint cell population, and subsequent loss of the ongoing effector response. Vaccination approaches aimed at the development of Tint populations may prove effective against pathogens that lead to chronic infection.

etoc Blure

Chu et al. show that ongoing presentation of an immunodominant pathogen-derived antigen sustains a proliferative CD8+ T cell subset with a phenotype that combines features of memory and effector T cells, thus revealing the source of functional CD8+ effector T cells that control

[5]Correspondence to: hamletchu.berkeley@gmail.com (H.H.C.) or erobey@berkeley.edu (E.A.R.).

Author Contributions: H.H.C. designed and performed experiments, analyzed data, and wrote the manuscript. E.A.R. designed experiments, analyzed data, and wrote the manuscript. J.P.G., G.L., and C.M-P. performed mathematical modeling and statistical analyses. S-W.C., N.B., A.T., and N.S. provided critical research tools.

All authors have no competing financial interest.

persistent infections. This intermediate subset continuously generates short-lived effector T cells and contributes to memory and effector T cell homeostasis.

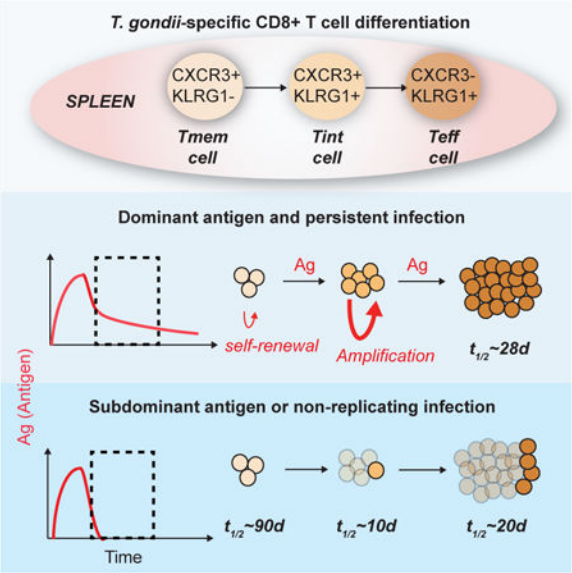

Introduction

CD8+ T cells provide protection against intracellular pathogens through a division of labor involving antigen-experienced effector and memory T cells. This process has been extensively examined in models of acute infection, in which pathogen-specific naïve CD8+ T cells rapidly expand and differentiate in response to signals from antigen and other environmental cues (Arens and Schoenberger, 2010; Jameson and Masopust, 2009). Upon pathogen clearance, short-lived effector T (Teff) cells die from apoptosis and a long-lived population of memory T (Tmem) cells remains (Joshi et al., 2007; Zehn et al., 2009). Long-lasting memory following acute infection is mediated by a stem cell-like population within the Tmem cell compartment that can self-renew or differentiate to generate new Teff cells upon secondary challenge (Gattinoni et al., 2011; Graef et al., 2014).

While the generation of T_{mem} cells has been a major focus of vaccine strategies, emerging evidence highlights the important protective function of an on-going effector T cell response (Masopust and Picker, 2012). For example, strong immune protection induced by a heterologous prime and boost strategy is due to a persistent effector T cell response (Jabbari and Harty, 2006; Masopust et al., 2006; Olson et al., 2013). Likewise, a prolonged effector T cell response is associated with protection in a promising cytomegalovirus (CMV) vector-based vaccine for simian immunodeficiency virus (SIV) (Hansen et al., 2009). Effector T cell responses are generally maintained by ongoing exposure to antigen (Mackay et al., 2012; Nelson et al., 2013); however, in many settings, persistent antigen leads to T cell exhaustion. Indeed, much of our knowledge regarding T cell responses to persistent infections comes from models in which pathogen control is incomplete and T cells become functionally impaired over time (Virgin et al., 2009; Wherry, 2011). Therefore, the cellular

mechanisms that maintain long-lasting effective control of persistent pathogens are not well understood.

Mouse cytomegalovirus (MCMV) infection is an important experimental model for understanding ongoing CD8+ effector T cell responses. Studies of MCMV infection in mice revealed continuous generation of Teff cells from an antigen-experienced progenitor population with a memory-like phenotype (Snyder et al., 2008) and a requirement for ongoing antigen presentation to maintain the CD8+ effector response (Snyder et al., 2011; Torti et al., 2011). One complicating feature of the MCMV infection model is the late expansion of certain CD8+ T cell specificities, a phenomenon termed “memory inflation” (Karrer et al., 2003). An additional complexity is the dominant protective role of NK cells in the C57BL/6 (B6) strain of mice (Vidal and Lanier, 2006). As a result, this model has not allowed for dissection of the developmental pathway that leads to continuous CD8+ effector generation *in vivo*. Hence, there is a pressing need for new mouse infection models to investigate the mechanism of CD8+ effector maintenance during controlled persistent infection.

A key to maintaining effective CD8+ T cell control of persistent intracellular pathogens is the host major histocompatibility complex (MHC) locus. For example, the ability to generate effective T cell responses to human immunodeficiency virus (HIV) is strongly linked to MHC-class I (MHC-I) polymorphisms that affect peptide binding (International et al., 2010; Kosmrlj et al., 2010). Moreover, HIV “elite controllers”, individuals who remain disease free without anti-viral therapy, often harbor highly functional CD8+ T cells specific for viral peptides presented by protective allelic forms of MHC-I (Almeida et al., 2007; Horton et al., 2006). Thus, an ideal experimental model for effective control of persistent infection may rely on particular combinations of host MHC-I and pathogen-derived antigenic peptides that can elicit unusually long lasting CD8+ T cell responses, along with a pathogen that has evolved to persist in the face of immune control.

We considered that infection of a resistant mouse strain by the intracellular protozoan parasite, *Toxoplasma gondii*, might provide such an ideal experimental model. *T. gondii* elicits a strong CD8+ T cell response, establishes life-long persistence in their mammalian hosts, and often produces asymptomatic infection. Moreover, mice harboring the MHC-I molecule L^d exhibit particularly effective control of the parasite due to an immunodominant CD8+ T cell response directed against the parasite protein, GRA6 (Blanchard et al., 2008; Brown et al., 1995). In contrast, mice without the protective L^d MHC-I molecule develop a chronic, progressive infection associated with dysfunctional T cell responses (Bhadra et al., 2011). Interestingly, both mouse MHC-I L^d, and human MHC-I alleles associated with elite HIV control, share key polymorphic amino acids in the peptide-binding site, and exhibit limited peptide binding capacity (Kosmrlj et al., 2010; Narayanan and Kranz, 2013). Thus, parasite infection in resistant mice shares a number of features of HIV elite control, including an atypical MHC-I allele that confers strong protection, a dominant CD8+ T cell response, and persistent but asymptomatic infection.

Here we examine the mechanisms that contribute to the effective anti-*T. gondii* CD8+ T cell response in genetically resistant mice. We showed that persisting antigen presentation drives

continuous production of highly functional Teff cells without a contraction phase. Using a combination of the effector marker, killer cell lectin-like receptor G1 (KLRG1), and the chemokine receptor CXCR3, we identified three subsets of antigen-experienced CD8+ T cells whose numbers were maintained over time by balanced proliferation, differentiation, and cell death. In addition to a relatively quiescent, memory-like population, and a terminally differentiated Teff cell population, we also identified a metabolically active intermediate population with hybrid memory and effector characteristics, and demonstrated that this population is strongly dependent on persistent antigen for survival, proliferation and differentiation. Our results revealed that effective CD8 T cell control of a persistent pathogen was maintained by a division of labor in which an intermediate T cell subset allowed for efficient and flexible generation of Teff cells in response to changing amounts of antigen, while Tmem cells provided for long-term maintenance of the response.

Results

CD8+ GRA6:L^d-specific T cell response to *T.gondii* exhibited immunodominance, lack of a contraction phase, and persistent effector response

Strong immune protection against the persistent intracellular protozoan parasite *T. gondii* in genetically resistant mice is linked to the MHC-I allele L^d and presentation of a single antigenic peptide derived from the parasite dense granule protein, GRA6 (Blanchard et al., 2008). We compared the anti-GRA6:L^d response to subdominant CD8+ T cell responses specific for peptides derived from parasite proteins GRA4 and ROP5 (Frickel et al., 2008; Grover et al., 2014) using F1 (H-2^{bxd}) mice orally infected with tissue cysts generated from the type II *T. gondii* strain, *Prugniaud* (Pru). Infected cells in both the draining mesenteric lymph nodes (MLN) and spleen peaked at 7 days after infection and were undetectable by day 21. We detected a low but persistent amount of *T. gondii* DNA in the brain beginning 11 days after oral infection (Figure 1A), reflecting the ability of *T. gondii* to establish chronic infection by encysting in the brain (Ferguson et al., 1989). In spite of parasite persistence, infected hosts did not show any sign of illness at >6 months post infection (data not shown), confirming the resistance of mice expressing the L^d allele of MHC-I (Brown et al., 1995).

To compare multiple CD8+ T cell populations from the same animal, we used fluorochrome-labeled peptide-MHC-I (pMHC-I) tetramers and flow cytometry. At day 21 after infection, GRA6:L^d-specific CD8+ T cells represented ∼20% of total CD8+ T cells, and were 100-fold more abundant than the subdominant GRA4:L^d- and ROP5:D^b-specific T cells (Figure 1B). At day 11, the subdominant T cells expanded 40-200 fold relative to their numbers at day 3, whereas splenic GRA6:L^d-specific T cells expanded ∼10,000 fold to $\sim 5\times10^5$ cells/spleen during the same time period, reaching a peak of $\sim10^6$ cells/spleen at 21 days post infection (Figure 1C). GRA6:L^d-specific T cells peaked at day 21 in the brain and persisted to at least day 200 after infection, while the subdominant T cells were 100-fold less numerous (Figure 1C). The majority of brain GRA6:L^d-specific T cells were not labeled by intravenous injection of CD45.1 antibody, indicating they resided in the brain parenchyma, and exhibited a phenotype consistent with tissue-resident memory T cells (Figure S1A and S1B) (Wakim et al., 2010). *T. gondii*-specific T cells in the spleen remained at peak numbers throughout the chronic phase of infection in spite of the sharp decline in parasite load

(Figure 1A and 1C). Hence, the *T. gondii*-specific CD8+ T cell response in resistant mice is characterized by rapid expansion of a single T cell specificity, and maintenance of large parasite-specific T cell population without a contraction phase.

While the loss of T cell effector function, termed T cell exhaustion, is observed in many chronic infections (Virgin et al., 2009), GRA6:L^d-specific T cells from chronically infected mice exhibited potent *in vivo* killing activity and produced large amounts of interferon (IFN) γ and tumor necrosis factor (TNF) α simultaneously upon brief *ex vivo* restimulation (Figure 1D and 1E). T cells specific for subdominant parasite antigens, in addition to their reduced numbers, produced less IFNγ and the majority failed to co-express TNFα (Figure 1E). GRA6:L^d-specific T cells also maintained higher expression of KLRG1, and lower expression of the memory marker CD62L as compared to the subdominant T cell responses (Figure 1F). *T. gondii*-specific T cells also lacked expression of the T cell exhaustion marker PD-1 during the chronic phase of infection, expressing it only transiently during the expansion phase (Figure 1F). Thus, the GRA6:L^d-specific T cell response is characterized by a large highly functional effector population that persists throughout chronic infection.

Persistent antigen presentation correlated with GRA6:L^d-specific T cell proliferation during the chronic phase of infection

The lack of a contraction phase and persistent effector function suggested that ongoing antigen presentation during the chronic phase of infection might drive the continuous generation of new Teff cells. To measure antigen presentation *in vivo*, we transferred naïve GRA6:L^d-specific transgenic T cells (TG6) (Figure S2) into previously infected mice and assessed their proliferation 3 days after transfer (Figure 2A). Substantial proliferation was observed when naïve TG6 T cells were transferred into mice that had been infected 140 days earlier with Pru strain parasites, but not in mice infected with a parasite strain that lacks the GRA6 epitope (Figure 2B). Thus, in spite of parasite clearance from secondary lymphoid organs (Figure 1A), GRA6 antigen presentation persisted late into chronic infection.

We also observed that 5-10% of total GRA6:L^d-specific cells in chronically infected mice were in cell cycle, based on expression of the proliferation marker Ki67, and overnight *in vivo* incorporation of the thymidine analog 5-ethynyl-2′-deoxyuridine (EdU) (Figure 2C and 2D). The decline of antigen presentation after initial infection correlated with the gradual reduction in the proportion of GRA6:L^d-specific T cells in cycle (Figure 2C), suggesting that persistent GRA6 antigen presentation drove the proliferation of a subset of GRA6:L^d-specific T cells during chronic infection.

GRA6:L^d-specific T cell immunodominance correlated with the predominance and persistence of a CXCR3+KLRG1+ population

Ongoing proliferation within the numerically stable GRA6:L^d-specific T cell population implies that the population size is maintained dynamically by continuous production of new cells balanced by cell loss. To investigate these population dynamics, we examined the composition of the dividing and non-dividing GRA6:L^d-specific T cell populations in more detail.

The GRA6:L^d-specific T cell response did not appear to be maintained by precursor population with a classic central memory phenotype (Sallusto et al., 1999), since antigen experienced GRA6:L^d specific T cells were uniformly CCR7-CD62L- (Figure S3A). In addition, while the combination of markers often used to distinguish effectors from memory precursors (KLRG1 and CD127)(Joshi et al., 2007) divided the population into three subsets, the proliferating population was equally distributed between these subsets (Figure S3B and S3C). In contrast, the combination of KLRG1 and CXCR3 revealed a KLRG1+CXCR3+ population that was highly enriched for proliferating cells (Figure S3B and S3C).

We noted that the T cell subsets defined by CXCR3 and KLRG1 differ in their proportions between dominant GRA6 and subdominant GRA4 and ROP5 specificities (Figure 3A). In particular, the GRA6:L^d-specific T cells consistently contained a higher proportion of CXCR3+KLRG1+ cells (Figure 3A and 3B). Moreover, the CXCR3+KLRG1+ subset of the GRA6:L^d-specific population persisted throughout infection, whereas the CXCR3+KLRG1+ subset in the GRA4:L^d and ROP5:D^b-specific T cells exhibited a marked decline between days 10-42 of infection and became barely detectable by day 60 after infection (Figure 3A and 3B). Thus, GRA6:L^d-specific T cell immunodominance correlates with the predominance and stability of the CXCR3+KLRG1+ population.

Recent thymic emigrants (RTEs) contribute to the stability of the antigen-specific CD8+ T responses in some persistent infections (Snyder et al., 2008; Vezys et al., 2006). To examine the role of RTEs in maintaining the GRA6-specific T cell population, we transferred a small number of naïve TG6 T cells into congenic recipients before oral infection, and enumerated TG6 cells over the course of infection. All three subsets defined by CXCR3 and KLRG1 expression demonstrated similar kinetics to the endogenous GRA6:L^d-specific T cells, including the lack of a contraction phase (Figure 3C). These data indicate that a stable GRA6-L^d-specific T cell population can be maintained over time without contribution from recent thymic emigrants.

The CXCR3+KLRG1+ subset had both memory and effector cell characteristics

To better characterize the populations defined by CXCR3 and KLRG1 expression, we performed flow cytometric analysis of GRA6:L^d-specific CD8+ T cells from chronically infected mice. CXCR3+KLRG1+ cells incorporated the largest amount of EdU after an overnight labeling, consistent with their Ki67 staining (Figure 4A, Figure S3B and S3C), and confirming that most proliferating cells were found within this subset. The CXCR3+KLRG1+ cells also contained the largest proportion of cells expressing the nutrient uptake receptors, CD71 and CD98 (Figure 4A) implying that they are more metabolically active. CXCR3+KLRG1+ cells expressed relatively low amounts of the anti-apoptotic molecule Bcl-2 (Figure 4B) and high amounts of the effector marker Blimp-1, but also expressed a memory-associated phenotype of CD122+, $CD27^{hi}CD43^{lo}$ (Hikono et al., 2007), and $Eomes^{hi}$ (Banerjee et al., 2010) (Figure 4C). *In vitro* cytotoxicity assays on sorted populations (Figure S3D to S3E) demonstrated that the CXCR3-KLRG1+ subset harbored the strongest cytotoxicity, followed by the CXCR3+KLRG1+ subset, while the CXCR3+KLRG1- subset exhibited minimal killing capacity (Figure S3F). Thus, the CXCR3

and KLRG1 gating strategy subdivided anti-*T. gondii* CD8+ T cells into three subsets of distinct functions and phenotypes, and identified a proliferative CXCR3+KLRG1+ subset with both memory and effector cell characteristics.

Lineage relationship and antigen dependence of the subsets defined by CXCR3 and KLRG1 expression

We next sorted GRA6:L^d-specific T cells from infected mice based on their CXCR3 and KLRG1 expression and followed their fates upon transfer into congenically marked infected recipients (Figure S4A). GRA6:L^d-specific CXCR3+KLRG1- and CXCR3+KLRG1+ cells proliferated and expanded 35 and 19 fold respectively between days 2 and 21 after transfer, whereas CXCR3-KLRG1+ cells exhibited little proliferation, and their numbers declined with a half-life of 28 days (Figure 5A and 5B). CXCR3+KLRG1- cells gave rise to all three subsets after transfer, whereas CXCR3+KLRG1+ cells gave rise only to CXCR3+KLRG1+ and CXCR3-KLRG1+ cells, and CXCR3-KLRG1+ cells maintained their phenotype (Figure 5B). Similar CXCR3 and KLRG1 profiles were obtained upon transfer of subsets into T and B cell deficient (*rag*$^{-/-}$) infected mice, although both donor CXCR3+ subsets underwent greater expansion compared to transfer into wild type recipients (Figure S4B). These experiments support the lineage relationship of CXCR3+KLRG1- ➔ CXCR3+KLRG1+ ➔ CXCR3-KLRG1+, and confirm that CXCR3-KLRG1+ cells are terminally differentiated.

Upon transfer of sorted subsets into naïve recipients, all three groups maintained their CXCR3 and KLRG1 phenotypes, and exhibited little proliferation (Figure 5C). Based on the recovery of donor cells at days 2 and 21 post transfer, CXCR3+KLRG1- cells showed the greatest survival with a half-live of 89 days, whereas CXCR3+KLRG1+ and CXCR3-KLRG1+ subsets displayed half-lives of 10 and 20 days respectively (Figure 5D). These relative half-lives are consistent with the expression of anti-apoptotic protein Bcl-2, which is lowest in the shortlived CXCR3+KLRG1+ population (Figure 4B). These data suggest that antigen is required for differentiation and proliferation of both CXCR3 expressing subsets. Based on their developmental order, phenotype and functional properties, we hereafter refer to CXCR3+KLRG1- cells as Tmem cells, CXCR+KLRG1+ cells as Tint cells, and CXCR3-KLRG1+ cells as Teff cells.

Persistent antigen presentation prevented T cell contraction by sustaining a Tint cell population

The results from cell transfer experiments and the strong antigen-dependence of the Tint cells implied that maintenance of this population by residual antigen was key to preventing T cell contraction following activation and expansion. To further test this idea, we examined the GRA6:L^d specific response to irradiated parasites, which can invade host cells and trigger a CD8+ T cell response, but fail to establish chronic infection *in vivo* (Hiramoto et al., 2002). To allow for a similar infection in the acute phase, we used an intraperitoneal (i.p.) route of infection with either 10^6 irradiated parasites or 10^5 live parasites. Initial GRA6 antigen presentation and early T cell expansion were comparable after injection of either irradiated or live parasites (Figure 6A and 6B). However, while antigen remained high 42 days after infection of mice with live parasites, antigen dropped markedly by day 12 and was undetectable at day 42 post-infection in mice injected with irradiated parasites (Figure 6A).

GRA6:L^d-specific T cells in mice infected i.p. with live parasites exhibited ongoing proliferation and no contraction phase (Figure 6B and C), similar to the results obtained from orally infected mice (Figure 3). In contrast, the sharp drop in antigen presentation in mice infected with irradiated parasites correlated with a marked reduction in the proportion of Ki67+ cells with an 80% loss of total GRA6:L^d-specific T cells between day 12 and day 21 (Figure 6B and C). While all T cell subsets declined during the contraction phase, the greatest reduction in cell number (20 fold) occurred in the Tint cell subset (Figure 6D and 6E). These data are consistent with the relative half-lives of the three populations following transfer into naïve mice (Figure 5D), and confirm that Tint cells are particularly dependent on persistent antigen for survival and proliferation.

We considered that a steep decline in presentation of the subdominant antigens could help to explain the loss of Tint cells amongst T cells responding to these antigens (Figure 3A and 3B). To test this idea, we examined *in vivo* presentation of the subdominant antigen ROP5, by transferring naïve T cells from ROP5:D^b-specific TCR transgenic mice (termed TR5 mice, Figure S5) into mice at different times post infection. Unlike the gradual reduction observed for the GRA6 antigen (Figure 6F and Figure 2C), presentation of the ROP5 antigen dropped sharply between days 13 to 50, corresponding to loss of Tint cells during this time window (Figure 6F). These data further support the importance of persistent antigen and Tint cells in maintaining an ongoing T cell response, and also help to explain the immunodominance of the GRA6:L^d-specific T cell population.

Mathematical modeling illustrated the role of the Tint cell subset in sustaining a robust effector T cell response

The ability of Tmem cells, but not Tint cells, to replenish all 3 subsets and survive in the absence of antigen implies that Tmem cells support the long-term maintenance of the GRA6:L^d-specific effector response, while Tint cells provide short-term amplification of the response. Consistent with this notion, Tint cells in chronically infected mice exhibited a relatively high proliferation rate, whereas Tmem cells were relatively quiescent (Figure 4A).

To further explore the roles of Tmem and Tint cells in maintaining the ongoing effector T cell response, we considered two alternative models. In one model, Tmem cells can divide to either produce another Tmem cell (self-renewal) or differentiate directly into a non-dividing Teff cell (Figure 7A). A second model includes Tint cells that can divide to produce another Tint cell (amplification) or can differentiate into a non-dividing Teff cell (Figure 7B and Figure 5A, see also Experimental Procedures). In both models, we assumed that Teff cells disappeared with a constant death rate of 0.027 cells/day (i.e. 2.7% of total Teff cells died each day) based on the cell transfer experiments in Figure 4B.

We first used model 1 to explore the range of Tmem cell self-renewal and differentiation rates that allowed for the observed overall rate of Teff cell production (2.5×10^6 Teff cells from 10^5 Tmem cells at steady state) (Figure 3B). By varying Tmem cell self-renewal and differentiation rates ($\lambda1$ and $\xi1$, respectively), we found that the self-renewal rate $\lambda1$ had to be greater than 0.3 cells/day to generate 2.5×10^6 Teff cells at steady state (Figure 7C). This value is incompatible with the observed low rate of proliferation of Tmem cells (i.e. 6% of the Tmem cells were labeled with EdU in every 14 hours, or 0.1 cells/day, see also Figure

4A). Moreover, increasing the differentiation rate to approach the self-renewal rate led to a sharp decline in the number of effectors, due to depletion of Tmem cells (Figure 7C and data not shown).

To evaluate the plausibility of model 2, we varied the Tint cell amplification and differentiation rates ($\lambda 2$ and $\xi 2$, respectively) while leaving the remaining parameters set at control values estimated from available experimental data (Table S1, see also Experimental Procedures), and calculated the number of Teff cells at steady state (Figure 7D). We observed that an amplification rate ($\lambda 2$) of 0.5 cells/day or greater allowed for the generation of 2.5×10^6 T_{eff} cells at steady state (Figure 7D), in line with observed rate of proliferation of Tint cells (i.e. 29% EdU-labeled cells in 14 hours, or 0.5 cells/day, see also Figure 4A). Moreover, unlike model 1, in which increasing the Tmem cell differentiation rate $\xi 1$ led to a precipitous drop in Teff cell production (Figure 7C), increasing the differentiation rate $\xi 2$ for model 2 led to reduced but sustained Teff cell production (Figure 7D). We also observed that the theoretical time course generated using model 2 and control parameters (Table S1A) correlated well with the experimental data derived from both the steady state cell number and cell transfer experiments (Figure 7E, Figure 3, and Figure 5A). These data suggest how Tint cells can allow for rapid and robust production of Teff cells, and can modulate the rate of differentiation of Teff cells without depleting a key progenitor population needed to sustain the response over the long-term.

Discussion

An ongoing T cell effector response is key to protective T-cell based vaccines, as well as natural resistance to persistent intracellular pathogens such as HIV (Masopust and Picker, 2012). However, the mechanisms that maintain robust T cell effector responses are largely unknown, due in part to the lack of appropriate mouse infection models. Here we show that persistent, asymptomatic *T. gondii*-infection in genetically resistant (H-2^d) mice gives rise to a robust immunodominant CD8+ effector response that is maintained over time without a contraction phase, and without any signs of functional exhaustion. We investigated the cellular mechanisms that maintain this effector response, revealing a division of labor in which a relatively quiescent and long-lived memory population (Tmem cells) gives rise to terminally differentiated effector cells (Teff cells) via a proliferative, antigen-sensitive intermediate population (Tint cells). Our data provide insight into the cellular dynamics that maintain robust ongoing CD8+ effector T cell responses, and highlight the importance of an amplifying Tint cell population to generate adequate numbers of new Teff cells in response to changing pathogen load, while preserving a long-lived population of Tmem cells.

Achieving a stable, asymptomatic standoff between an intracellular pathogen and an ongoing effector T cell response requires both a pathogen that is able to occupy a long-term niche in the host, and a T cell response with appropriate specificity to provide highly effective immune control. With regard to the latter, it is intriguing to note that MHC-I variants associated with HIV elite control, and the MHC-I molecule L^d that presents the immunodominant parasite antigen GRA6, share structural features including atypical peptide binding properties (International et al., 2010; Kosmrlj et al., 2010; Narayanan and Kranz, 2013). For the GRA6 antigen, a number of other factors contribute to efficient

antigen presentation, including the secretion pattern of the antigenic protein within the invaded host cell, and the location of the epitope within the precursor protein (Feliu et al., 2013; Grover et al., 2014; Lopez et al., 2015). Thus, both features of a particular antigenic protein and presentation by an atypical MHC-I molecule may contribute to an unusually protective CD8+ T cell response.

In addition to the protective pressure exerted by T cells, the ability of certain pathogens to adopt a relatively latent form in the host also contributes to the stable standoff between pathogen and host immune response. We showed that continued presence of the parasite, leading to persistent antigen presentation, is required to prevent T cell contraction and maintain robust effector T cell responses. *T. gondii* is able to achieve long-term persistence by converting to a relatively dormant, cyst-forming stage in the brain of its infected host (Montoya and Liesenfeld, 2004). Likewise the ability of β-herpesvirues, including cytomegalovirus (CMV), to adopt a latent form in mammalian host cells, leading to a continuous source of antigen, and perhaps helping to explain the remarkable potency and longevity of effector T cell responses elicited by a CMV-based vaccine against SIV in non-human primates (Hansen et al., 2009). Heterologous prime-boost vaccination strategies can generate long-lived effector responses without persistent infection (Jabbari and Harty, 2006; Masopust et al., 2006; Olson et al., 2013), perhaps due to long-lived antigen depots that persist after viral clearance (Leon et al., 2014; Turner et al., 2007).

A large body of literature using acute infection models has subdivided antigen-experienced CD8+ T cells into effector and memory populations based on cell surface markers including CCR7, CD62L, CD127 (IL7Rα), and KLRG1 (Joshi et al., 2007; Sallusto et al., 1999). Interestingly, the distinction between central memory (CCR7+CD62L+) and effector memory (CCR7-CD62L-) (Sallusto et al., 1999) does not appear to be relevant in this infection model, since antigen experienced GRA6:L^d-specific CD8+ T cells were uniformly low for CCR7 and CD62L expression. This included the memory-like CXCR3+KLRG1- population that could give rise to all other subsets and was long-lived in the absence of antigen. Moreover, CD127, which has been used in conjunction with KLRG1 to distinguish memory precursor versus short-lived effectors (Joshi et al., 2007), does not appear to be useful marker in this infection model. Rather, transition from CXCR3+KLRG1+ Tint cell to CXCR3-KLRG1+ Teff cell phenotype correlated with the loss of proliferation and terminal differentiation of effector cells. Interestingly, Yap and colleagues observed cycling T cells of CXCR3+KLRG1+ phenotype in an acute *T. gondii* vaccination model, and found that Teff cell terminal differentiation correlated with CXCR3 downregulation in an interleukin-12 and IFNγ dependent manner (Shah et al., 2015). Together with our results, these findings suggest that the precise timing of TCR and cytokine or chemokine signals may be important for regulating T cell amplification and effector differentiation during infection by modulating the number of CXCR3+KLRG1+ Tint cells.

Our modeling studies point to the role of Tint cells in maintaining an ongoing effector T cell response. Without Tint cells, Tmem cells would need to proliferate extensively to keep up with the demand for new Teff cell output. Moreover, if increasing antigen amounts were to drive more rapid differentiation into Teff cells, this would lead to the depletion of the Tmem cell population and eventually the collapse of the T cell response. Hence the presence of Tint

cells allows for rapid production of new Teff cells while maintaining a relatively quiescent Tmem cell population when antigen remains constant, and provides extra capacity for increasing Teff cell differentiation in response to increasing antigen.

One interesting feature of Tint cells is their high expression of the T-box transcription factor Eomes. Eomes, and the related transcription factor T-bet play partially redundant roles in CD8+ T cells, although Eomes also plays unique roles in the maintenance of memory and exhausted T cells (Banerjee et al., 2010; Intlekofer et al., 2005; Paley et al., 2012). Interestingly, high Eomes expression is also associated with a proliferative subset of CD8+ T cells found in some HIV-infected individuals, and correlates with effective viral control (Simonetta et al., 2014). Moreover, Eomes is highly expressed in intermediate neural progenitor cells, where it is required for the maintenance of the intermediate population and ongoing neurogenesis (Hodge et al., 2012). Understanding the precise role of Eomes in maintaining robust CD8+ T cell effector responses during persistent infection is an important area for future investigation.

In summary, we used a controlled persistent *T. gondii* infection model to delineate the cellular mechanism that sustains a long-term CD8+ Teff cell response. We identified a T cell intermediate subset that provides for efficient effector cell output, and is responsive to antigen. Approaches to manipulate the numbers of Tint cells, perhaps via regulated release of antigen, may improve the efficacy of current vaccine regimens by sustaining robust effector T cell responses, while preserving a stable population of Tmem cells.

Experimental Procedures

Detailed experimental procedures can be found in the Supplemental Information section.

Animals

Mouse strains and the procedures for generating the TG6 and TR5 TCR transgenic mice are described in **Supplemental Experimental Procedures**. All mice were bred in UC Berkeley animal facility and were used with the approval of the Animal Care and Use Committee of the University of California.

Infection and flow cytometry

Mice were orally or intraperitoneally (i.p.) infected with the type II Prugniuad-tomato-OVA strain (Pru)(Chtanova et al., 2008) or the type III CEP strain (Grover et al., 2014) *T. gondii*. Detailed protocols for infection and flow cytometric staining of cell suspensions from the spleen, lymph nodes, and brains of infected mice are described in **Supplemental Experimental Procedures**.

ex vivo cytokine production assay

Splenocytes from mice 60-140 days post infection were cultured with GRA6 peptide or GRA4 and ROP5 peptide (Peptide2.0 Inc., Chantilly, VA) in media for 4 hours with the presence of protein secretion block (eBioscience). Cells were then harvested for surface and intracellular antibody staining before flow cytometry analysis.

GRA6 and ROP5 antigen presentation detection *in vivo*

To provide a sensitive method to detect ongoing antigen presentation, we adopted a detection method in Turner et al (Turner et al., 2007). In brief, we harvested from lymph nodes (LNs) and spleen of CD45.2+ TG6 or TR5 mice $H2^{bxd}$ background, labeled with the cell proliferation dye eFluor 450 (eBioscience, San Diego, CA), transferred cells containing 10^5 TG6 or TR5 cells into previously CD45.1+ infected mice, and examined proliferation dye dilution 3 days later. Relative antigen presentation is expressed as the % of donor TG6 or TR5 cells that have diluted proliferation dye (proliferation dye^{low}) 3 days after transfer.

Adoptive transfer and cell sorting

To expand TG6 cells *in vivo*, cells were harvested from lymph nodes (LNs) and spleen of CD45.2+ TG6 mice on $H2^{bxd}$ background and transferred into CD45.1+ naïve F1 recipients at 10,000-100,000 CD8+ TG6 cells/mouse one day before infection. Detailed cell sorting procedures are described in **Supplemental Experimental Procedures**

In vitro cytotoxicity assay

Sorted subsets of CXCR3+KLRG1-, CXCR3+KLRG1+, and CXCR3-KLRG1+CD8+ TG6 cell subsets were obtained from infected mice as described above for adoptive transfer. Each subset was cultured with GRA6-peptide-pulsed and PBS-pulsed splenocytes from congenically marked naïve F1 mice at 1:5:5 ratio. The GRA6-peptide-pulsed and PBS-pulsed splenocytes were distinguished by different intensity of CFSE labeling (5-(and-6)-Carboxyfluorescein Diacetate, Succinimidyl Ester, Invitrogen). Cytotoxicity was assessed by the loss of the GRA6-peptide-pulsed splenocytes relative to the PBS-pulsed control after 18 hours of culture.

In vivo cytotoxicity assay

Splenocytes from F1 naïve mice were labeled with cell proliferation dye eFluor 450 at four different levels of intensity. Each labeled population was then pulsed with either 1μM of GRA6, GRA4, ROP5-pepitdes (Peptide2.0 Inc.) or PBS for 1 hour at 37°C. Pulsed cells were then washed twice and mixed at 1:1:1:1 ratio with 10^6 cells from each population. Cell mixture was injected intravenously into chronically infected mice and harvested 18 hours later.

Mathematical modeling and Bayesian statistical analysis

To illustrate the role of Tint cells in Teff cell production and maintenance, two modes were considered. Model 1 follows the linear order: Tmem cell (CXCR3+KLRG1-, called ×1) ➔ Teff cell (CXCR3-KLRG1+, called ×3); **1b)** Model 2 follows the linear order: Tmem cell (CXCR3+KLRG1-, called ×1) ➔ Tint cell (CXCR3+KLRG1+, called ×2) ➔ Teff cell (CXCR3-KLRG1+, called ×3); Equations for the mathematical models are described in **Supplemental Experimental Procedures**. Figure 7C and 7D were generated in Mathematica (Wolfram, Champagne, IL) as a function of λ1 and ξ1 (Figure 7C) or λ2 and ξ 2 (Figure 7D). Figure 7E was generated in Python (PSF, Beaverton, OR).

To obtain a measure of the plausibility of the model and the control parameters, we performed a Bayesian statistical calibration of the model using the available data (steady state spleen T cell numbers and cell transfer data in Figure 3 and Figure 5). Analysis was performed in Matlab (Mathworks, Natick, MA). Detailed method is described in **Supplemental Experimental Procedures**.

Code Availability

The mathematical equations for the number of cells of population ×3 at steady state (Figure 7C and 7D), as a function of (model 1) $\lambda 1$ and $\xi 1$ and of (model 2) $\lambda 2$ and $\xi 2$ are provided as a Mathematica code in **Supplemental File**. The mathematical model to obtain the time course for the dynamics of the three populations (model 2 and Figure 7E) is provided as a numerical Python code in **Supplemental File**. Source code used for Bayesian statistical analysis is available upon request.

Additional Statistical Analysis for Experimental Data

All p-values were calculated in Prism (GraphPad, La Jolla, CA). Detail procedures are described in **Supplemental Experimental Procedures**.

Supplementary Material

Refer to Web version on PubMed Central for supplementary material.

Acknowledgments

We thank C. Kang for generating TG6 transgenic mice, K. Taylor and I. Chou for expert technical assistance, the NIH Tetramer Core for peptide-MHC tetramers, H. Nolla and A. Valero for cell sorting, M. Jenkins (U of Minnesota), M. Prlic (Fred Hutchson Cancer Research Center), and members of the Robey Lab for helpful comments. This work was supported by grants from the American National Institutes of Health P01 AI065831 (E.A.R. and N.S.), R01 AI065537 and AI093132 (E.A.R.); the American Heart Association and the California Institute for Regenerative Medicine (H.H.C.); the Human Frontier Science Program (N.B.); the UK's National Centre for Replacement, Refinement and Reduction of Animals in Research NC/K001280/1 (J.P.G.), the Leeds Fund for International Research Collaborations (G.L. and C.M-P.), the Biotechnology and Biological Sciences Research Council BB/F003811/1 (G.L. and C.M-P.) and BB/G023395/1 (C.M-P).

References

Almeida JR, Price DA, Papagno L, Arkoub ZA, Sauce D, Bornstein E, Asher TE, Samri A, Schnuriger A, Theodorou I, et al. Superior control of HIV-1 replication by CD8+ T cells is reflected by their avidity, polyfunctionality, and clonal turnover. J Exp Med. 2007; 204:2473–2485. [PubMed: 17893201]

Arens R, Schoenberger SP. Plasticity in programming of effector and memory CD8 T-cell formation. Immunol Rev. 2010; 235:190–205. [PubMed: 20536564]

Banerjee A, Gordon SM, Intlekofer AM, Paley MA, Mooney EC, Lindsten T, Wherry EJ, Reiner SL. Cutting edge: The transcription factor eomesodermin enables CD8+ T cells to compete for the memory cell niche. J Immunol. 2010; 185:4988–4992. [PubMed: 20935204]

Bhadra R, Gigley JP, Weiss LM, Khan IA. Control of Toxoplasma reactivation by rescue of dysfunctional CD8+ T-cell response via PD-1-PDL-1 blockade. Proc Natl Acad Sci U S A. 2011; 108:9196–9201. [PubMed: 21576466]

Blanchard N, Gonzalez F, Schaeffer M, Joncker NT, Cheng T, Shastri AJ, Robey EA, Shastri N. Immunodominant, protective response to the parasite Toxoplasma gondii requires antigen processing in the endoplasmic reticulum. Nat Immunol. 2008; 9:937–944. [PubMed: 18587399]

Brown CR, Hunter CA, Estes RG, Beckmann E, Forman J, David C, Remington JS, McLeod R. Definitive identification of a gene that confers resistance against Toxoplasma cyst burden and encephalitis. Immunology. 1995; 85:419–428. [PubMed: 7558130]

Chtanova T, Schaeffer M, Han SJ, van Dooren GG, Nollmann M, Herzmark P, Chan SW, Satija H, Camfield K, Aaron H, et al. Dynamics of neutrophil migration in lymph nodes during infection. Immunity. 2008; 29:487–496. [PubMed: 18718768]

Feliu V, Vasseur V, Grover HS, Chu HH, Brown MJ, Wang J, Boyle JP, Robey EA, Shastri N, Blanchard N. Location of the CD8 T cell epitope within the antigenic precursor determines immunogenicity and protection against the Toxoplasma gondii parasite. PLoS Pathog. 2013; 9:e1003449. [PubMed: 23818852]

Ferguson DJ, Hutchison WM, Pettersen E. Tissue cyst rupture in mice chronically infected with Toxoplasma gondii. An immunocytochemical and ultrastructural study. Parasitol Res. 1989; 75:599–603. [PubMed: 2771928]

Frickel EM, Sahoo N, Hopp J, Gubbels MJ, Craver MP, Knoll LJ, Ploegh HL, Grotenbreg GM. Parasite stage-specific recognition of endogenous Toxoplasma gondii-derived CD8+ T cell epitopes. J Infect Dis. 2008; 198:1625–1633. [PubMed: 18922097]

Gattinoni L, Lugli E, Ji Y, Pos Z, Paulos CM, Quigley MF, Almeida JR, Gostick E, Yu Z, Carpenito C, et al. A human memory T cell subset with stem cell-like properties. Nat Med. 2011; 17:1290–1297. [PubMed: 21926977]

Graef P, Buchholz VR, Stemberger C, Flossdorf M, Henkel L, Schiemann M, Drexler I, Hofer T, Riddell SR, Busch DH. Serial transfer of single-cell-derived immunocompetence reveals stemness of CD8(+) central memory T cells. Immunity. 2014; 41:116–126. [PubMed: 25035956]

Grover HS, Chu HH, Kelly FD, Yang SJ, Reese ML, Blanchard N, Gonzalez F, Chan SW, Boothroyd JC, Shastri N, Robey EA. Impact of regulated secretion on antiparasitic CD8 T cell responses. Cell reports. 2014; 7:1716–1728. [PubMed: 24857659]

Hansen SG, Vieville C, Whizin N, Coyne-Johnson L, Siess DC, Drummond DD, Legasse AW, Axthelm MK, Oswald K, Trubey CM, et al. Effector memory T cell responses are associated with protection of rhesus monkeys from mucosal simian immunodeficiency virus challenge. Nat Med. 2009; 15:293–299. [PubMed: 19219024]

Hikono H, Kohlmeier JE, Takamura S, Wittmer ST, Roberts AD, Woodland DL. Activation phenotype, rather than central- or effector-memory phenotype, predicts the recall efficacy of memory CD8+ T cells. J Exp Med. 2007; 204:1625–1636. [PubMed: 17606632]

Hiramoto RM, Galisteo AJ, do Nascimento N, de Andrade HF Jr. 200 Gy sterilised Toxoplasma gondii tachyzoites maintain metabolic functions and mammalian cell invasion, eliciting cellular immunity and cytokine response similar to natural infection in mice. Vaccine. 2002; 20:2072–2081. [PubMed: 11972976]

Hodge RD, Nelson BR, Kahoud RJ, Yang R, Mussar KE, Reiner SL, Hevner RF. Tbr2 is essential for hippocampal lineage progression from neural stem cells to intermediate progenitors and neurons. The Journal of neuroscience : the official journal of the Society for Neuroscience. 2012; 32:6275–6287. [PubMed: 22553033]

Horton H, Frank I, Baydo R, Jalbert E, Penn J, Wilson S, McNevin JP, McSweyn MD, Lee D, Huang Y, et al. Preservation of T cell proliferation restricted by protective HLA alleles is critical for immune control of HIV-1 infection. J Immunol. 2006; 177:7406–7415. [PubMed: 17082660]

International HIVCS, Pereyra F, Jia X, McLaren PJ, Telenti A, de Bakker PI, Walker BD, Ripke S, Brumme CJ, Pulit SL, et al. The major genetic determinants of HIV-1 control affect HLA class I peptide presentation. Science. 2010; 330:1551–1557. [PubMed: 21051598]

Intlekofer AM, Takemoto N, Wherry EJ, Longworth SA, Northrup JT, Palanivel VR, Mullen AC, Gasink CR, Kaech SM, Miller JD, et al. Effector and memory CD8+ T cell fate coupled by T-bet and eomesodermin. Nat Immunol. 2005; 6:1236–1244. [PubMed: 16273099]

Jabbari A, Harty JT. Secondary memory CD8+ T cells are more protective but slower to acquire a central-memory phenotype. J Exp Med. 2006; 203:919–932. [PubMed: 16567385]

Jameson SC, Masopust D. Diversity in T cell memory: an embarrassment of riches. Immunity. 2009; 31:859–871. [PubMed: 20064446]

Joshi NS, Cui W, Chandele A, Lee HK, Urso DR, Hagman J, Gapin L, Kaech SM. Inflammation directs memory precursor and short-lived effector CD8(+) T cell fates via the graded expression of T-bet transcription factor. Immunity. 2007; 27:281–295. [PubMed: 17723218]

Karrer U, Sierro S, Wagner M, Oxenius A, Hengel H, Koszinowski UH, Phillips RE, Klenerman P. Memory inflation: continuous accumulation of antiviral CD8+ T cells over time. J Immunol. 2003; 170:2022–2029. [PubMed: 12574372]

Kosmrlj A, Read EL, Qi Y, Allen TM, Altfeld M, Deeks SG, Pereyra F, Carrington M, Walker BD, Chakraborty AK. Effects of thymic selection of the T-cell repertoire on HLA class I-associated control of HIV infection. Nature. 2010; 465:350–354. [PubMed: 20445539]

Leon B, Ballesteros-Tato A, Randall TD, Lund FE. Prolonged antigen presentation by immune complex-binding dendritic cells programs the proliferative capacity of memory CD8 T cells. J Exp Med. 2014; 211:1637–1655. [PubMed: 25002751]

Lopez J, Bittame A, Massera C, Vasseur V, Effantin G, Valat A, Buaillon C, Allart S, Fox BA, Rommereim LM, et al. Intravacuolar Membranes Regulate CD8 T Cell Recognition of Membrane-Bound Toxoplasma gondii Protective Antigen. Cell reports. 2015; 13:2273–2286. [PubMed: 26628378]

Mackay LK, Wakim L, van Vliet CJ, Jones CM, Mueller SN, Bannard O, Fearon DT, Heath WR, Carbone FR. Maintenance of T cell function in the face of chronic antigen stimulation and repeated reactivation for a latent virus infection. J Immunol. 2012; 188:2173–2178. [PubMed: 22271651]

Masopust D, Ha SJ, Vezys V, Ahmed R. Stimulation history dictates memory CD8 T cell phenotype: implications for prime-boost vaccination. J Immunol. 2006; 177:831–839. [PubMed: 16818737]

Masopust D, Picker LJ. Hidden memories: frontline memory T cells and early pathogen interception. J Immunol. 2012; 188:5811–5817. [PubMed: 22675215]

Montoya JG, Liesenfeld O. Toxoplasmosis. Lancet. 2004; 363:1965–1976. [PubMed: 15194258]

Narayanan S, Kranz DM. The same major histocompatibility complex polymorphism involved in control of HIV influences peptide binding in the mouse H-2Ld system. J Biol Chem. 2013; 288:31784–31794. [PubMed: 24064213]

Nelson RW, McLachlan JB, Kurtz JR, Jenkins MK. CD4+ T cell persistence and function after infection are maintained by low-level peptide:MHC class II presentation. J Immunol. 2013; 190:2828–2834. [PubMed: 23382562]

Olson JA, McDonald-Hyman C, Jameson SC, Hamilton SE. Effector-like CD8(+) T cells in the memory population mediate potent protective immunity. Immunity. 2013; 38:1250–1260. [PubMed: 23746652]

Paley MA, Kroy DC, Odorizzi PM, Johnnidis JB, Dolfi DV, Barnett BE, Bikoff EK, Robertson EJ, Lauer GM, Reiner SL, Wherry EJ. Progenitor and terminal subsets of CD8+ T cells cooperate to contain chronic viral infection. Science. 2012; 338:1220–1225. [PubMed: 23197535]

Sallusto F, Lenig D, Forster R, Lipp M, Lanzavecchia A. Two subsets of memory T lymphocytes with distinct homing potentials and effector functions. Nature. 1999; 401:708–712. [PubMed: 10537110]

Shah S, Grotenbreg GM, Rivera A, Yap GS. An extrafollicular pathway for the generation of effector CD8(+) T cells driven by the proinflammatory cytokine, IL-12. Elife. 2015; 4

Simonetta F, Hua S, Lecuroux C, Gerard S, Boufassa F, Saez-Cirion A, Pancino G, Goujard C, Lambotte O, Venet A, Bourgeois C. High eomesodermin expression among CD57+ CD8+ T cells identifies a CD8+ T cell subset associated with viral control during chronic human immunodeficiency virus infection. J Virol. 2014; 88:11861–11871. [PubMed: 25100841]

Snyder CM, Cho KS, Bonnett EL, Allan JE, Hill AB. Sustained CD8+ T cell memory inflation after infection with a single-cycle cytomegalovirus. PLoS Pathog. 2011; 7:e1002295. [PubMed: 21998590]

Snyder CM, Cho KS, Bonnett EL, van Dommelen S, Shellam GR, Hill AB. Memory inflation during chronic viral infection is maintained by continuous production of short-lived, functional T cells. Immunity. 2008; 29:650–659. [PubMed: 18957267]

Torti N, Walton SM, Brocker T, Rulicke T, Oxenius A. Non-hematopoietic cells in lymph nodes drive memory CD8 T cell inflation during murine cytomegalovirus infection. PLoS Pathog. 2011; 7:e1002313. [PubMed: 22046127]

Turner DL, Cauley LS, Khanna KM, Lefrancois L. Persistent antigen presentation after acute vesicular stomatitis virus infection. J Virol. 2007; 81:2039–2046. [PubMed: 17151119]

Vezys V, Masopust D, Kemball CC, Barber DL, O'Mara LA, Larsen CP, Pearson TC, Ahmed R, Lukacher AE. Continuous recruitment of naive T cells contributes to heterogeneity of antiviral CD8 T cells during persistent infection. J Exp Med. 2006; 203:2263–2269. [PubMed: 16966427]

Vidal SM, Lanier LL. NK cell recognition of mouse cytomegalovirus-infected cells. Curr Top Microbiol Immunol. 2006; 298:183–206. [PubMed: 16329187]

Virgin HW, Wherry EJ, Ahmed R. Redefining chronic viral infection. Cell. 2009; 138:30–50. [PubMed: 19596234]

Wakim LM, Woodward-Davis A, Bevan MJ. Memory T cells persisting within the brain after local infection show functional adaptations to their tissue of residence. Proc Natl Acad Sci U S A. 2010; 107:17872–17879. [PubMed: 20923878]

Wherry EJ. T cell exhaustion. Nat Immunol. 2011; 12:492–499. [PubMed: 21739672]

Zehn D, Lee S, Bevan M. Complete but curtailed T-cell response to very low-affinity antigen. Nature. 2009; 458:211–214. [PubMed: 19182777]

Highlights

- *T. gondii* infection in resistant mice recapitulates aspects of HIV elite control.

- A novel T intermediate (Tint) subset maintains a long-lived effector response.

- Persistent presentation of the dominant antigen maintains the Tint cell subset.

- Targeting Tint cells may lead to improved treatment of persistent infections.

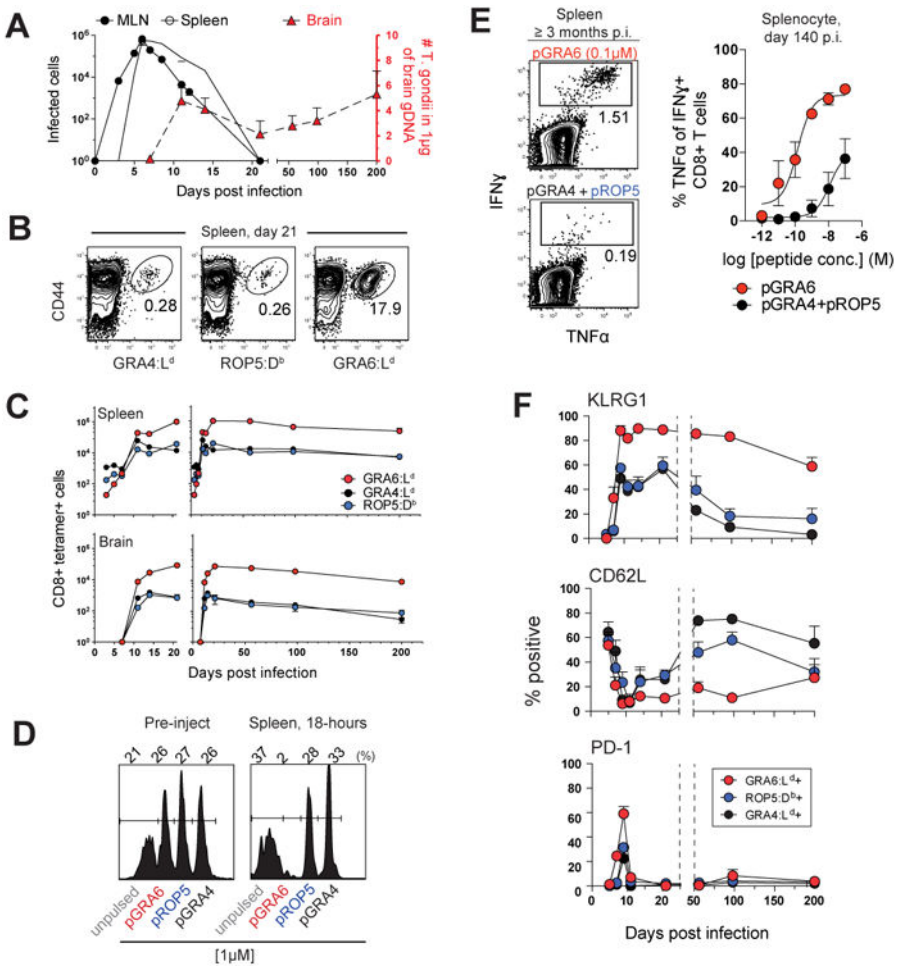

Figure 1. CD8+ GRA6:L^{d}-specific T cell response to *T.gondii* exhibited immunodominance, lack of a contraction phase, and persistent effector responses

(A) Kinetics of parasite burden in F1 H2^{bxd} mice after oral infection with Pru strain parasites expressing RFP. Parasite loads in the mesenteric lymph node (MLN, filled circles) and in the spleen (open circles) are shown as numbers of RFP+ infected cells. Parasite load in the brain were determined by semi-quantitative PCR and is expressed as number of parasite genomes per 1µg of host genomic DNA (red triangles). **(B)** Representative flow cytometry plots showing GRA4:L^{d}-, ROP5:D^{b}-, or GRA6:L^{d}-tetramer expression on gated CD8+ T cells from the spleens of mice day 21 after infection. Numbers represent the percent of tetramer+ cells out of splenic CD8+ T cells. **(C)** Number of GRA4:L^{d}-(black circles), ROP5:D^{b}- (blue circles), or GRA6:L^{d}-(red circles)-tetramer-specific CD8+ T cells in the spleen (top) and brain (bottom) at the indicated time points post infection. **(D)** *In vivo* cytotoxicity of anti-*T. gondii* CD8+ T cells. Representative histograms showing the CFSE staining of target cell populations pre-transfer, or 18 hours after transfer into day 90 chronically infected mice. Target cells were individually pulsed with 1µM of indicated peptides and labeled with a different concentration of fluorescent dye, then mixed at 1:1:1:1 ratio just prior to injection into mice. Values are the percent of each donor population before and after transfer. **(E)** Left panel shows representative flow cytometry plots of IFNγ and TNFα in splenic CD8+ T cells from day 140 chronically infected mice after *ex vivo*

stimulation with indicated peptides for 4 hours. Values are the percent of IFNγ positive cells out of CD8+ T cells. Right panel shows the percentage of TNF*a* producing cells amongst IFN*γ*+CD8+ T cells following stimulation with a serial dilution of GRA6 (red) or a mixture of GRA4 and ROP5 peptides (black). **(F)** Kinetics of KLRG1, CD62L, and PD-1 expression. Values are the percent positive cells out of each of the splenic GRA4:L^d-(black circles), ROP5:D^b- (blue circles), and GRA6:L^d- (red circles) tetramer+ CD8+ T cell population from mice at the indicated times post infection. Graph in **(A-C, F)** are summary of 3-5 independent experiments with total N equal to 4-10 mice at each time point. **(D, E)** are representative of 3 independent experiments with total N=5 mice 2-4 months post infection. Graphs in **(A, C and F)** display mean ±S.E.M. See also Figure S1.

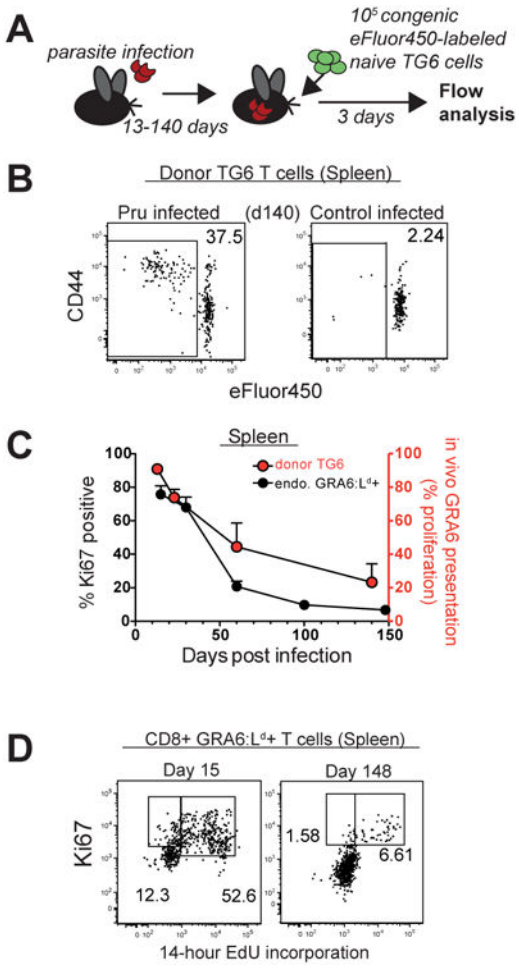

Figure 2. Kinetics of antigen presentation *in vivo* correlated with GRA6:L^d-specific T cell proliferation

(A) Strategy for quantifying of *in vivo* GRA6 antigen presentation in infected mice. (See also Experimental Procedures). **(B)** Representative flow cytometry plots of donor TG6 T cells recovered 3 days after injection into day 140 post infection mice. Control mice were infected with CEP strain parasites, which express an allelic form of GRA6 that lacks the relevant T cell epitope. **(C)** GRA6 antigen presentation *in vivo* in mice that were infected for the indicated times (red circles). Percentage of Ki67+ cells out of endogenous splenic GRA6:L^d-tetramer+ CD8+ T cells in orally infected mice (black circles) are shown for comparison. **(D)** Representative flow cytometry plots showing Ki67 expression and 14-hour *in vivo* EdU labeling by gated splenic GRA6:L^d-specific CD8+ splenic T cells at day 15 or day 148 after infection. Panels in **(B and D)** are representative of 3 independent experiments with total N=5-6 mice per group. Graph in **(C)** is summary of 3 independent experiments with total N equal to 4-5 mice at each time point. Values are percent of cells in the indicated gates or quadrants. See also Figure S2.

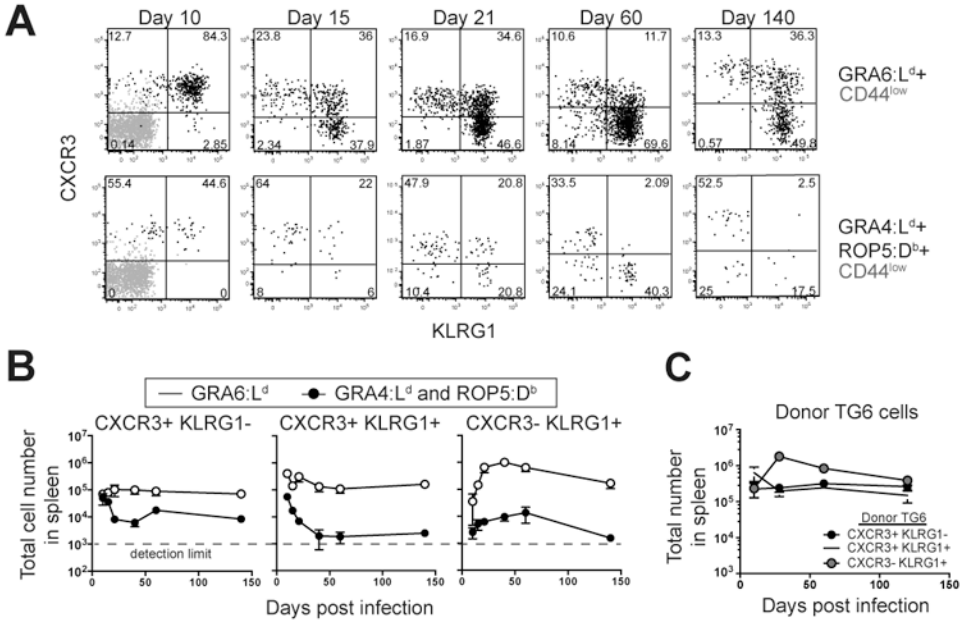

Figure 3. Predominance and stability of a CXCR3+KLRG1+ population within the GRA6:L^{d}-specific T cell subset

(A) Representative flow cytometry plots showing CXCR3 vs. KLRG-1 expression of splenic GRA6:L^{d}- and GRA4:L^{d} and ROP5:D^{b}-tetramer+ CD8+ T cells at the indicated times after infection. Naïve CD44^{low} CD8+ T cells are shown in grey for reference. **(B)** Total numbers of splenic CXCR3+KLRG1-, CXCR3+KLRG1+ and CXCR3-KLRG1+ cells within the GRA6:L^{d}- (open circles) or GRA4:L^{d} and ROP5:D^{b}-(filled circles) tetramer+ CD8+ T cells over time after infection. The dashed line indicates the detection limit of this assay at 10^{3} cell/spleen. **(C)** Total number of splenic donor TG6 CXCR3+KLRG1-, CXCR3+KLRG1+ and CXCR3-KLRG1+ cells at different times post infection. Panels in **(A)** are representative of 3-6 independent experiments with total N=5-8 mice at each time point. Graphs in **(B and C)** are summary of 3-5 independent experiments with total N equal to 3-8 mice at each time point, except in **(B)**, day 140 post infection (2 independent experiment with total N equal to 2 mice). Graphs in **(B and C)** display mean±S.E.M. See also Figure S3.

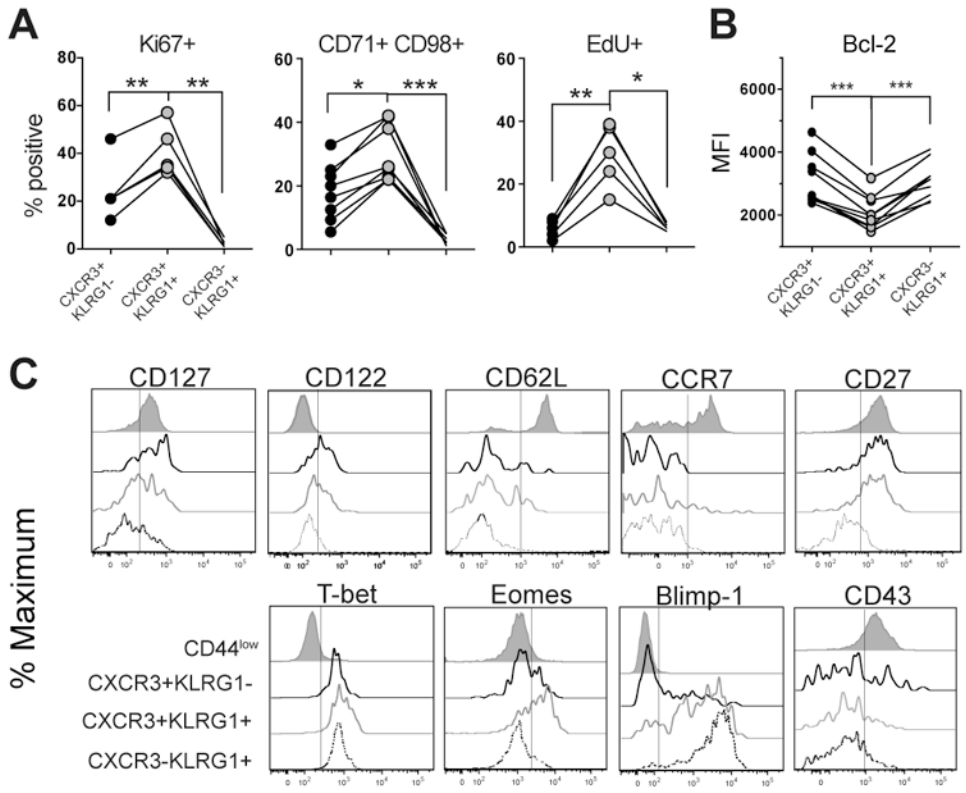

Figure 4. The CXCR3+KLRG1+ subset was enriched with proliferating cells and had characteristics of memory and effector cells

(A and B) Flow cytometric analysis of splenic GRA6:L^d-tetramer+ CD8+ T cells from infected mice. Data points from the same animal are indicated by connecting lines. Each symbol indicates value from an individual mouse. **(A)** The percentages of Ki67+ (left), CD71+CD98+ (middle) and EdU+ (right) cells within the indicated subset defined by CXCR3 and KLRG1 expression 60 days after infection. **(B)** The mean fluorescent intensity (MFI) of Bcl-2 staining in the indicated splenic GRA6:L^d-tetramer+ subsets at ≥ 40 days after infection. **(C)** Representative histograms showing expression of memory and effector T cell markers in the indicated splenic GRA6:L^d-specific subsets 60 days after infection. All panels are summary of 3-6 independent experiments per group. $*P < 0.05$, $**P < 0.01$, and $***P < 0.001$ (one-way ANOVA with Tukey's post test).

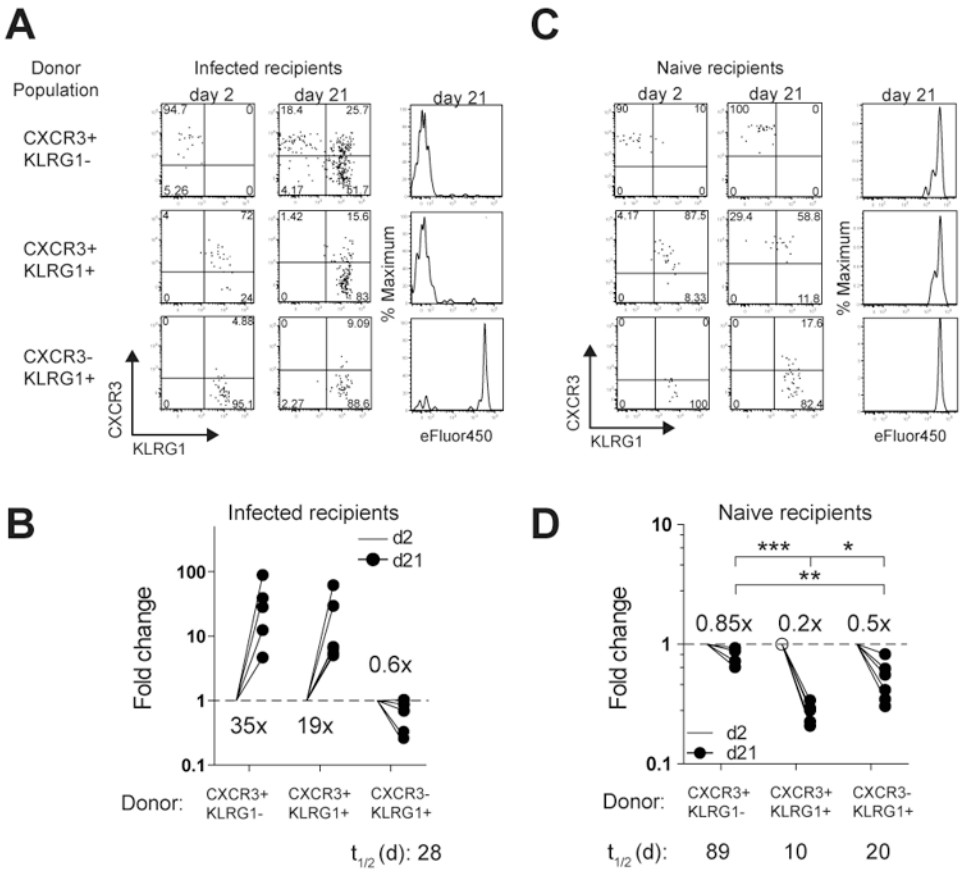

Figure 5. Lineage relationship and antigen dependence of the T cell subsets defined by CXCR3 and KLRG1 expression

(A and C) Representative flow cytometry plots showing CXCR3 and KLRG1 expression and proliferation dye dilution on sorted donor TG6 subsets 2 days or 21 days after transfer into ≥ day 21 infected **(A)** or naive **(C)** recipients. **(B and D)** Fold change in the number of the indicated donor-derived subsets between 2-21 days after transfer into infected **(B)** or naive **(D)** recipients. Each filled circle represents the value from an individual recipient at day 21 normalized to the mean value of day 2 post transfer from all experiments (open circle). Numbers inside the graphs indicate the mean fold change for each subset between day 2 and day 21. *$P < 0.05$, **$P < 0.01$, and ***$P < 0.001$ (one-way ANOVA with Tukey's post test). All panels are representative of 3-4 independent experiments. Total N of each panel is indicated in the corresponding scattered plots. **(B, D)** Half-lives of each subset ($t_{1/2}$) were calculated by: $t_{1/2}$ =19days * ln(2)/ln(N_{day2}/N_{day21}), N = donor TG6 cell number recovered. See also Figure S4.

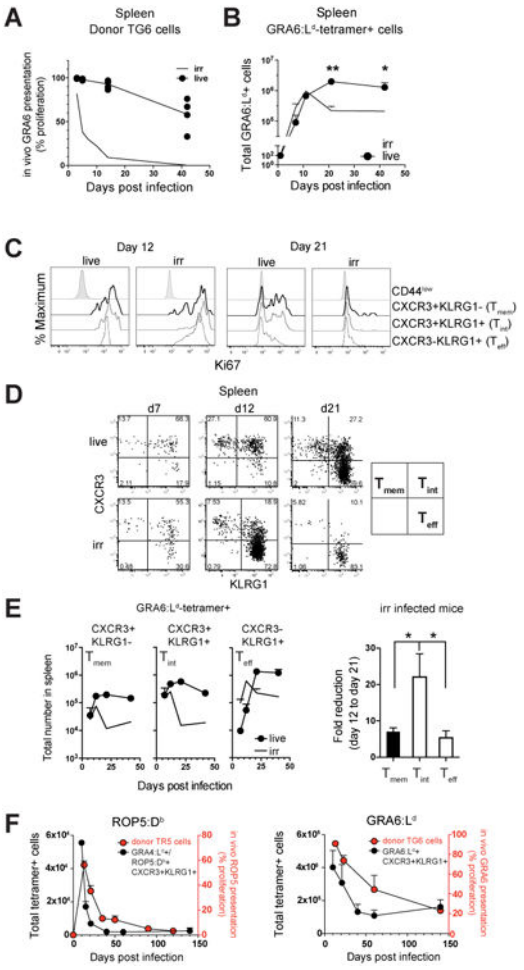

Figure 6. Persistent antigen presentation prevented T cell contraction by sustaining the Tint cell population

(A-E) Mice were infected i.p. with either 10^5 live ("live", filled circles) or 10^6 irradiated ("irr", open circles) and analyzed at the indicated times by flow cytometry **(A)** Kinetics of splenic GRA6 antigen presentation *in vivo* (measured as described in Figure 2A). **(B)** Splenic GRA6:L^d-tetramer+ CD8+ T cell number. **(C)** Representative histograms showing Ki67 expression in the indicated subset of splenic GRA6:L^d-specific T cells. **(D)** Representative flow cytometry plots showing CXCR3 and KLRG1 expression of splenic GRA6:L^d-tetramer+ CD8+ T cells. **(E)** Kinetics of the indicated splenic GRA6:L^d-tetramer+ CD8+ T cell subsets (left). Fold reduction in each T cell subset between day 12 and 21 in mice infected with irradiated *T. gondii*. (right) **(F)** ROP5 antigen presentation *in vivo* (red circles) in spleens of orally infected mice, measured as described in Figure 2A and Figure S5. Numbers of splenic CXCR3+KLRG1+ cells (black circle) from Figure 3B are shown for comparison. Right panel shows comparable data for *in vivo* GRA6 antigen presentation and numbers of splenic GRA6:L^d-specific CXCR3+KLRG1+ T cells. GRA6 antigen presentation data is from Figure 2C, and is included here for comparison. Graph in **(A)** is summary of 2 independent experiments with total N equal to 3-4 mice at each time point. Each symbol indicates value from individual recipients. Graph in **(B)**, $*P = 0.043$ and $**P = 0.003$ (unpaired, two-tailed student t-test); Graph in **(E)**, $*P = 0.02$ (one-way ANOVA with

Tukey's post test). Graphs in **(B and E)** are summary of 3-4 independent experiments with total N equal to 4-7 mice at each time point. Panels in **(C, D, and F)** are representative of 3 independent experiments with total N=3-5 mice at each time point. Graphs in **(A, B, E and F)** display mean±S.E.M.

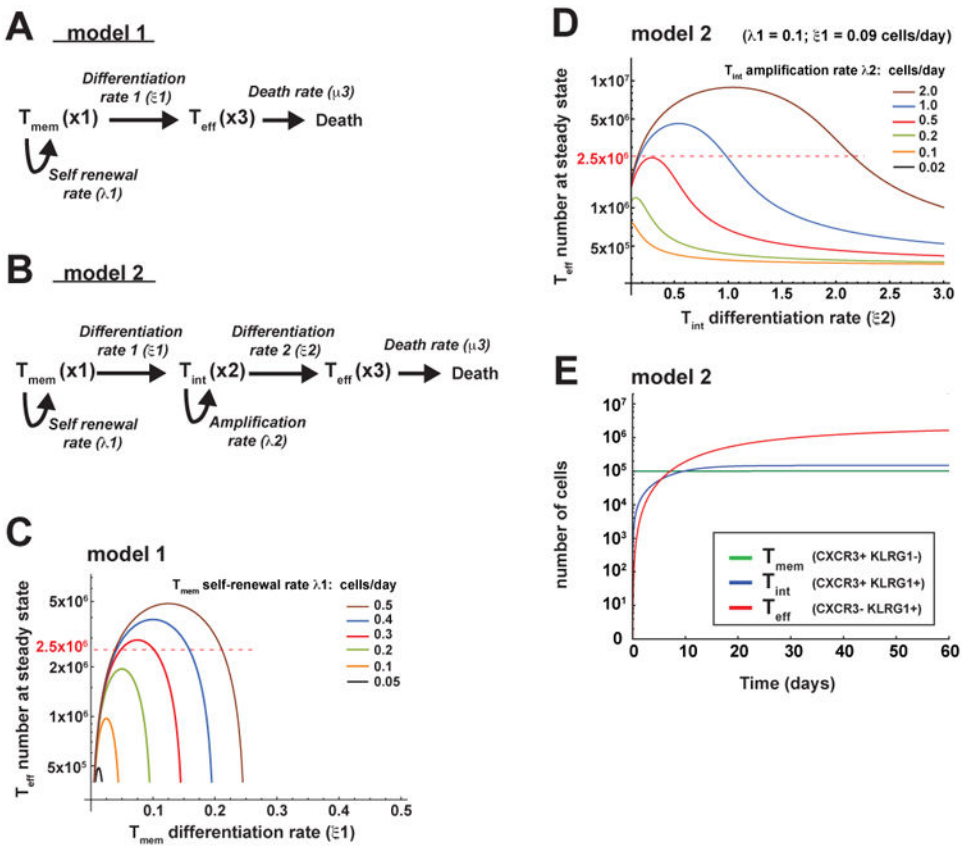

Figure 7. Mathematical modeling illustrated the role of the Tint subset in sustaining a robust effector T cell response

Mathematical models describing the population dynamics of the GRA6:L^d response with **(A)** or without **(B)** Tint cells. See also **Experimental Procedures** and **Supplemental Experimental Procedures** for details. **(C)** Dependence of Teff cell numbers at steady state on the Tmem cell self-renewal rate λ1 and differentiation rate ξ1, according to model 1. The remaining parameters were fixed at the control values (see also Table S1A). **(D)** Dependence of Teff cell numbers at steady state on the Tint cell amplification rate λ2 and differentiation rate ξ2, according to model 2. The remaining parameters were fixed at the control values (see also Table S1A). The red dashed line indicates the experimental value for number of Teff cells found in spleens of chronically infected mice. **(E)** Changes in numbers of Tmem, Tint, and Teff cells as a function of time starting with 10^5 Tmem cells using the model 2 in panel **(B)** and control parameters (see also Table S1A).